

Geometric Layouts of Qubits for New Lattice Codes

von
Dennis Huben

Bachelorarbeit in Physik

vorgelegt der
Fakultät für Mathematik, Informatik und Naturwissenschaften der
Rheinisch-Westfälischen Technischen Hochschule Aachen

im Juni 2012

angefertigt im
Institut für Quanteninformation
bei
Professor Dr. DiVincenzo

Contents

1	Abstract	5
2	Introduction	7
3	Circuit QED	13
4	A New Geometric Layout	17
5	Example of a Measurement Round in the Triangular Code	23
	Bibliography	27

1 Abstract

Quantum computers may be built along the lines of many different suggestions. However, it is not always obvious how those abstract ideas can be represented in a concrete form. This thesis looks at Bravyi's triangular code [2] and shows how it could be implemented.

Chapters 2 and 3 serve as a general introduction to quantum computing and circuit quantum electrodynamics (circuit QED). Chapter 4 presents a solution to the problem at hand and explains how the solution was obtained. Finally, chapter 5 gives an example of how this new layout can be used in error correcting procedures.

2 Introduction

A quantum computer is a computer which makes use of the laws of quantum mechanics. Whereas a bit in classical computation can only have one of two states (0 and 1), a qubit in a quantum computer can have a state $|\psi\rangle$ which is a superposition of the two: $|\psi\rangle = \alpha|0\rangle + \beta|1\rangle$, where α and β are complex numbers with $|\alpha|^2 + |\beta|^2 = 1$. Still, when the state of a qubit is measured, it will still always be either $|0\rangle$ or $|1\rangle$. The factors α and β indicate the probability that either of the states appears: $|\alpha|^2$ for state $|0\rangle$ and $|\beta|^2$ for state $|1\rangle$. One can imagine each possible state as a point on a unit-sphere, the so-called "Bloch sphere": Each state $|\psi\rangle$ can also be written as $|\psi\rangle = e^{i\gamma} (\cos(\theta/2)|0\rangle + e^{i\phi}\sin(\theta/2)|1\rangle)$. As the global phase $e^{i\gamma}$ has no physical meaning, knowledge of the real numbers ϕ and θ , identifying a point on the Bloch sphere, is sufficient to describe a state. [1]

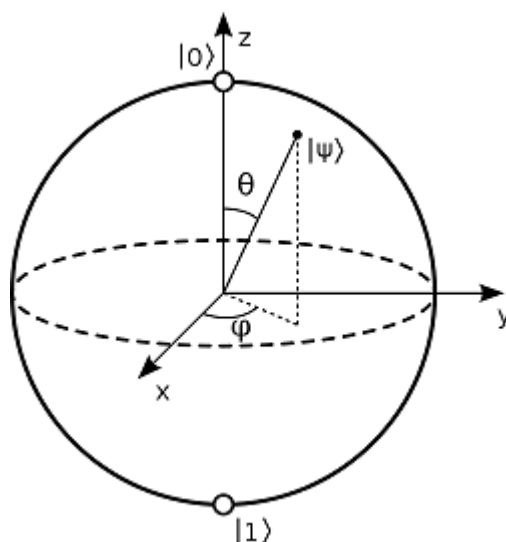


Figure 1: The Bloch sphere. From [3].

This, together with other quantum mechanical phenomena like entanglement, allows for algorithms to work differently than in a classical computer and can allow certain problems to be solved much faster. One example for this is the prime number factorization of arbitrarily large numbers. No classical algorithm is known with which this can be computed in polynomial time. That means that the number of steps required to find the prime factors grows very fast with the size of the number. On a quantum computer, Shor's algorithm can solve this problem in polynomial time, which is much more efficient than any classical algorithm. [1][6]

Computational operations are carried out by so-called "gates". One example for this is the X-gate, which is analogous to a classical NOT operation and maps the state $|\psi\rangle = \alpha|0\rangle + \beta|1\rangle$ to $|\bar{\psi}\rangle = \beta|0\rangle + \alpha|1\rangle$. If one looks at $|0\rangle$ and $|1\rangle$ as a base with

$$|0\rangle = \begin{pmatrix} 1 \\ 0 \end{pmatrix} \text{ and } |1\rangle = \begin{pmatrix} 0 \\ 1 \end{pmatrix},$$

all operations which can be performed have an associated matrix. To calculate the state of the qubit after passing through the gate you multiply the vector

$$\begin{pmatrix} \alpha \\ \beta \end{pmatrix},$$

describing the state $|\psi\rangle$, with the matrix. For example, the matrix for the X-gate is

$$X = \begin{pmatrix} 0 & 1 \\ 1 & 0 \end{pmatrix}.$$

Also very useful is the Z-gate,

$$Z = \begin{pmatrix} 1 & 0 \\ 0 & -1 \end{pmatrix}$$

which changes the sign of the $|1\rangle$ state, but leaves $|0\rangle$ untouched. There is only one condition for the matrix M to be a valid operator: It has to be unitary, which simply means that $M^\dagger M = I$.

Another example for a commonly used gate is the Hadamard gate, which can be described as a transition to another base: $|0\rangle$ becomes $\frac{1}{\sqrt{2}}(|0\rangle + |1\rangle)$ (or $|+\rangle$), and $|1\rangle$ becomes $\frac{1}{\sqrt{2}}(|0\rangle - |1\rangle)$ (or $|-\rangle$). In this base, the roles of X and Z Operators are reversed: A Z-gate changes $|+\rangle$ to $|-\rangle$ and vice versa, while an X-gate leaves $|+\rangle$ untouched and changes the sign of $|-\rangle$. The matrix corresponding to the Hadamard gate is

$$H = \frac{1}{\sqrt{2}} \begin{pmatrix} 1 & 1 \\ 1 & -1 \end{pmatrix}.$$

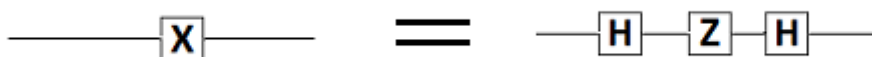


Figure 2: Applying a X-gate to a qubit is equivalent to applying in this order a Hadamard, a Z-gate and another Hadamard.

The X and Z-gates and the Hadamard are not only unitary, but additionally they are real and $M = M^T$, so that $M = M^\dagger$. From this it follows directly that the state doesn't change if you apply either of those gates to a state twice without any intermediate steps. You can see this from the matrices, as multiplying those matrices with themselves gives the 2x2 identity matrix.

Similarly to the gates mentioned before, there are gates which work on two qubits. Perhaps the most simple example of this is the "controlled-NOT", or CNOT, gate. Here, one qubit is the "control", while the other one is the "target". The control is left unchanged. If it is in the $|1\rangle$ state, a NOT-gate is applied to the target. If the control is in the $|0\rangle$ state, the target is left unchanged. Looking at this as vectors and matrices, where

$$|00\rangle = \begin{pmatrix} 1 \\ 0 \\ 0 \\ 0 \end{pmatrix}$$

means that both qubits are in the $|0\rangle$ state,

$$|01\rangle = \begin{pmatrix} 0 \\ 1 \\ 0 \\ 0 \end{pmatrix}$$

means that the states of the qubits are $|0\rangle$ for the control and $|1\rangle$ for the target, etc., the CNOT corresponds to the transformation matrix

$$\begin{pmatrix} 1 & 0 & 0 & 0 \\ 0 & 1 & 0 & 0 \\ 0 & 0 & 0 & 1 \\ 0 & 0 & 1 & 0 \end{pmatrix}.$$

The CNOT is an universal 2-qubit gate, which means that, together with certain 1-qubit gates, it is possible to perform every operation on two qubits with just a combination of CNOTs and those 1-qubit gates. Nevertheless, there are other important 2-qubit gates, for example the "controlled-Z", which maps every state to itself, except for $|11\rangle$, where it flips the sign, so $|11\rangle$ becomes $-|11\rangle$. This is equivalent to the matrix

$$\begin{pmatrix} 1 & 0 & 0 & 0 \\ 0 & 1 & 0 & 0 \\ 0 & 0 & 1 & 0 \\ 0 & 0 & 0 & -1 \end{pmatrix}.$$

As opposed to the CNot, the controlled-Z is a symmetrical gate: It does not matter which qubit is the control and which is the target.

1-qubit gates are carried out through rotations of the qubit state in the Bloch sphere. For example, to apply a Hadamard gate to a state, one can use a $\frac{\pi}{2}$ rotation about the y-axis followed by a π rotation about the x-axis. That this is correct can easily be confirmed by looking at the corresponding rotation matrices: Rotations about the y-axis, respectively the x-axis, are represented by the following matrices:

$$R_y(\theta) = \begin{pmatrix} \cos(\frac{\theta}{2}) & \sin(\frac{\theta}{2}) \\ -\sin(\frac{\theta}{2}) & \cos(\frac{\theta}{2}) \end{pmatrix}$$

$$R_x(\theta) = \begin{pmatrix} \cos(\frac{\theta}{2}) & -i \sin(\frac{\theta}{2}) \\ -i \sin(\frac{\theta}{2}) & \cos(\frac{\theta}{2}) \end{pmatrix}$$

Therefore,

$$R_y\left(\frac{\pi}{2}\right) \cdot R_x(\pi) = \frac{1}{\sqrt{2}} \begin{pmatrix} -i & -i \\ -i & i \end{pmatrix} = e^{-i\frac{\pi}{2}} \cdot \frac{1}{\sqrt{2}} \begin{pmatrix} 1 & 1 \\ 1 & -1 \end{pmatrix},$$

which is just the Hadamard gate except for a global phase $e^{-i\frac{\pi}{2}}$, which does not matter.

There are several unintuitive or at least non-obvious phenomena surrounding quantum computing. For example, one could want to copy the unknown state $|\psi\rangle = \alpha|0\rangle + \beta|1\rangle$ of a qubit onto another qubit, essentially "cloning" the first qubit. This is impossible though, other than in a few specialized cases. This is known as the "no-cloning theorem".

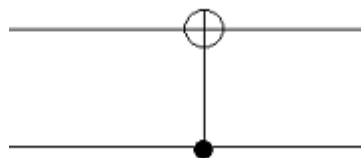


Figure 3: Symbol for the CNOT-gate. The bottom line represents the control qubit and the top line represents the target qubit.

Error correction is an important aspect of quantum computing. In classical computation, it is very unlikely that a bit switches from 0 to 1, or vice versa, because of the relatively large amount of energy which would be needed for this to happen. Due to the continuous nature of the state of qubits, in quantum computing small changes can easily become disruptive. One typical error which could happen is a bit flip, equivalent to the application of an X-gate. Another type of error would be a sign flip, where a state $\alpha |0\rangle + \beta |1\rangle$ becomes $\alpha |0\rangle - \beta |1\rangle$, analogous to a Z-gate. Because it is impossible to completely prevent the occurrence of these errors, error correction procedures have to be applied. A simple example would be using three qubits instead of one to detect bit flip errors in case the state of the qubit is supposed to be either $|0\rangle$ or $|1\rangle$. While it is now actually more likely that an error occurs, it is possible to detect it by measuring all three qubits. In case the qubits yield different measurement results, it is very likely that the result which is shared by two qubits is the "real" result, as it is very unlikely that two (or even all three) qubits encountered an error somewhere during the process. To detect different kinds of errors more sophisticated methods have to be used, which use for example 5, 7 or 9 qubits [1][6].

Qubits can be implemented physically through systems with two or more levels. In the case of a system with more than two levels, the non-computational levels are chosen in a way those states do not interfere with the computational levels. This is achieved for example in systems where the energy gap between the ground state and the first excited state is much different from the gap between the first and the second excited state. It is also important that the system has relatively large relaxation times. If the relaxation time would be short, the system would not preserve the state long enough to do useful operations.

3 Circuit QED

Circuit quantum electrodynamics allow a physical representation of qubits. Here, artificial atoms couple through transmission lines.

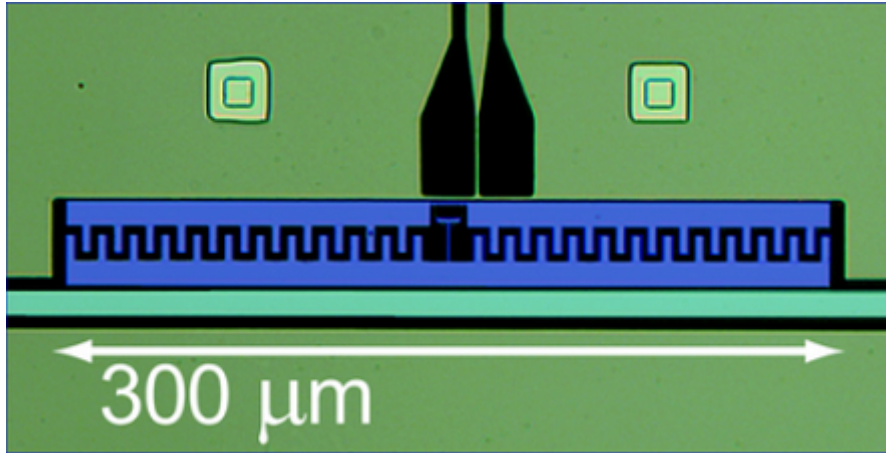


Figure 4: A transmon consisting of an interdigitated capacitor (blue) and a Josephson junction (black, in the center of the picture). There is a flux bias line leading to the transmon from the top. A transmission line (light green) runs next to the transmon. Image taken from [4].

A transmon is an example for such an artificial atom. It mainly consists of a Josephson junction, which works as a non-linear, tuneable inductance, and a capacitor. The non-linearity is of great help here, as the energy gap between the first and the second excited state is different enough from the energy gap between the ground state and the first excited state. Transmons have relaxation times in the order of magnitude of $10 \mu s$ [7] and a length of about $300 \mu m$. Typical transition frequencies are in the GHz range.

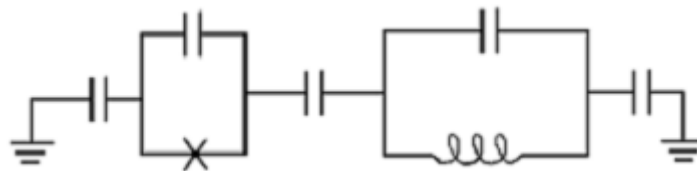


Figure 5: Circuit diagram of a transmon and a transmission line. On the left side is the transmon, consisting of a capacitor and a Josephson junction in parallel. The transmission line is represented through a capacitance and an inductance in parallel.

Flux bias lines make it possible to change the state of the transmon and couple it to other transmons. By changing the current which flows through the bias line, the

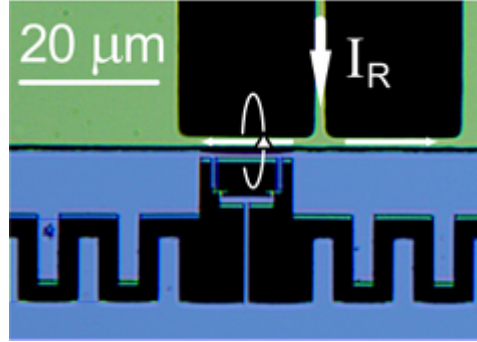


Figure 6: From [4]. The ending of the flux bias line and part of the transmon including the Josephson junction. The incoming current induces a variable magnetic field through the junction.

magnetic field in the Josephson junction changes as well, which allows variation of the transmon's transition frequency.

Transmission lines are realized through coplanar waveguides, essentially the 2-d analogue to a coaxial cable. They consist of a superconducting line with two dielectrics on the side, which are in turn next to grounded planes. Qubits on the same transmission line can be coupled to each other if they are both in resonance with each other.

Fig. 7 and 8 show how controlled-Phase gates are implemented. V_R is the voltage applied to the second qubit. Point I is where measurement and single-qubit operations, such as preparing the qubit to a certain state, happen. Here the transition frequency is at a maximum and is very different from the frequency of the other qubits and the cavity. If the voltage is changed so that the frequencies are brought closer together, interactions between the qubits can happen and the excitation can fluctuate between the different transmons. There is also an additional effect visible: When the two lines in the graph would cross, instead they do not cross. This is what happens at point III in Fig. 7 and is called an "avoided crossing". When an even higher voltage is applied at that point, the resonance frequency of the qubit the voltage is applied to remains roughly constant, and the frequency of the other qubit now starts to decline.

The feature which allows the execution of c-Phases and therefore also controlled-Z gates is visible in Fig. 8. Because of the avoided crossing between the non-computational state $|02\rangle$ and the computational state $|11\rangle$, the sum of the frequencies of $|01\rangle$ and $|10\rangle$ is different from $|11\rangle$. In the computational base, the phase gate looks like this:

$$U = \begin{pmatrix} 1 & 0 & 0 & 0 \\ 0 & e^{i\phi_{10}} & 0 & 0 \\ 0 & 0 & e^{i\phi_{01}} & 0 \\ 0 & 0 & 0 & e^{i\phi_{11}} \end{pmatrix},$$

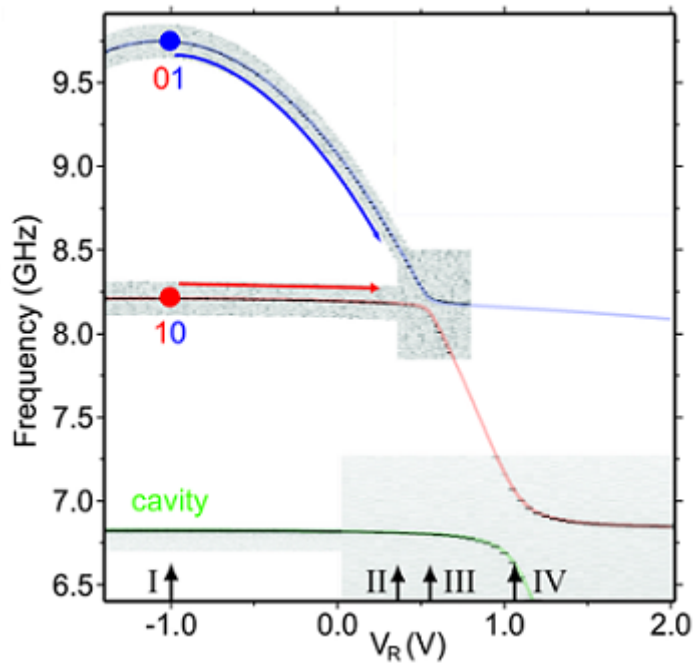


Figure 7: Adapted from [4]. Image showing the transition frequencies of the qubits against the voltage on the bias line. At point I single-qubit operations are performed. On point II phase gates can be executed. Points III and IV show avoided crossings.

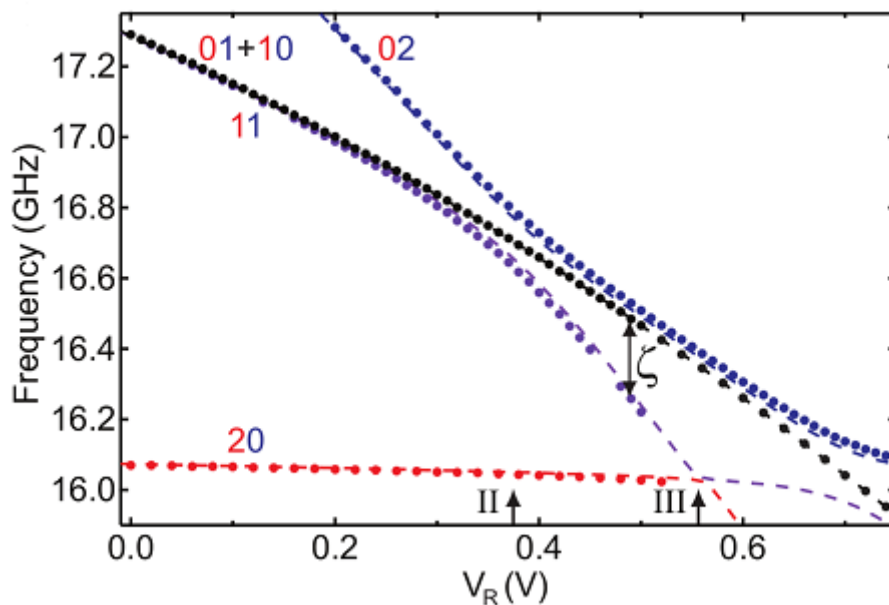


Figure 8: From [4]. Image showing the frequency gap ζ between the state $|11\rangle$ and the sum of $|01\rangle$ and $|10\rangle$ depending on the flux. One can see the avoided crossings between the non-computational state $|02\rangle$ and the computational state $|11\rangle$ and between $|20\rangle$ and $|11\rangle$.

where ϕ_{ab} signifies the phase the gate applies to the state $|ab\rangle$. If $\phi_{11} = \phi_{10} + \phi_{01} + \delta$, to apply a controlled-Z, one has to make it so that $\delta = \pi$ (or more generally $\delta = (2n + 1)\pi$, with an integer n). Then the phase gate U can also be written as

$$U = \begin{pmatrix} 1 & 0 & 0 & 0 \\ 0 & e^{i\phi_{10}} & 0 & 0 \\ 0 & 0 & 1 & 0 \\ 0 & 0 & 0 & e^{i\phi_{10}} \end{pmatrix} \begin{pmatrix} 1 & 0 & 0 & 0 \\ 0 & 1 & 0 & 0 \\ 0 & 0 & e^{i\phi_{01}} & 0 \\ 0 & 0 & 0 & e^{i\phi_{01}} \end{pmatrix} \begin{pmatrix} 1 & 0 & 0 & 0 \\ 0 & 1 & 0 & 0 \\ 0 & 0 & 1 & 0 \\ 0 & 0 & 0 & -1 \end{pmatrix},$$

which works as a controlled-Z gate on the two qubits. If one considers the frequency gap ζ in Fig. 8 to be constant in time, one just has to apply the pulse which moves the system to point II for a length τ , with $\zeta \cdot \tau = \pi$. More generally again, if $\zeta = \zeta(t)$, the following equation has to be satisfied: $\int \zeta(t) dt = (2n + 1)\pi$.

4 A New Geometric Layout

I based the layout on Bravyi's triangular code [2]. Here, each qubit taking part in the actual computations is grouped with four so-called "ancilla" qubits, and each ancilla is in turn coupled with three computational qubits. The ancillas can be measured to extract an error syndrome without disturbing the states of the computational qubits.

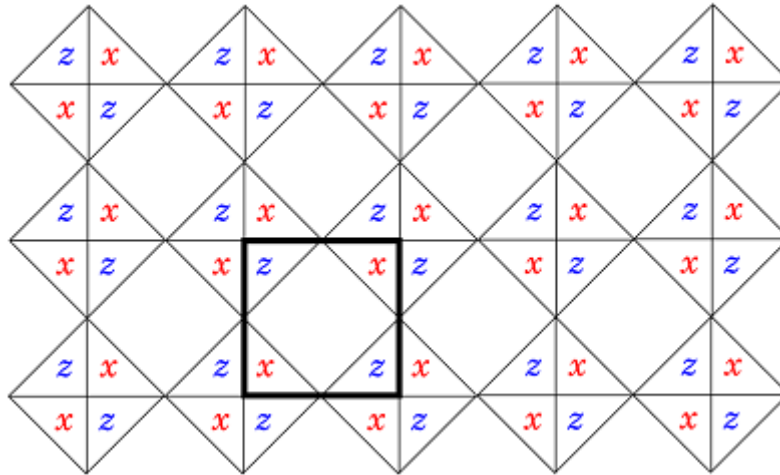


Figure 9: The Triangular code, taken from [2]. Computational qubits are on those points where four lines touch; for example, in the bold square there is a qubit in each corner and one qubit in the center of each side, for a total of eight qubits. "x" and "z" mark the position and type of the ancilla qubits, which are used for detection of errors. Each ancilla is next to three computational qubits and each computational qubit is next to four ancillas, two x and two z.

I designed the layout as a structure of transmon qubits and transmission lines adhering to the following rules:

1. Computational qubits need to have transmission lines connecting them to each of the four ancillas surrounding them.
2. On each transmission line there can be up to four qubits (computational and ancilla).
3. Each qubit should only be connected to two transmission lines.

It follows directly from rules 1 and 3 that at least two of the ancillas which belong to a qubit need to be on the same transmission line. From rule 2 you can see that there can be either two ancillas each on both the transmission lines, or there are three ancillas on the first and one ancilla on the second transmission line. The obvious way is to go with the first solution, because this allows another computational qubit on

those transmission lines. Now, each ancilla is already connected to two of the three qubits it needs connecting to. You can just add another transmission line from that ancilla to the missing computational qubit. As this would lead to that qubit having four transmission lines leading to it, two of those transmission lines each have to be merged, which results in two transmission lines leading from ancilla to ancilla, with a computational qubit in the middle. Each computational qubit is now connected to all four relevant ancillas. Abstractly, the layout looks like this:

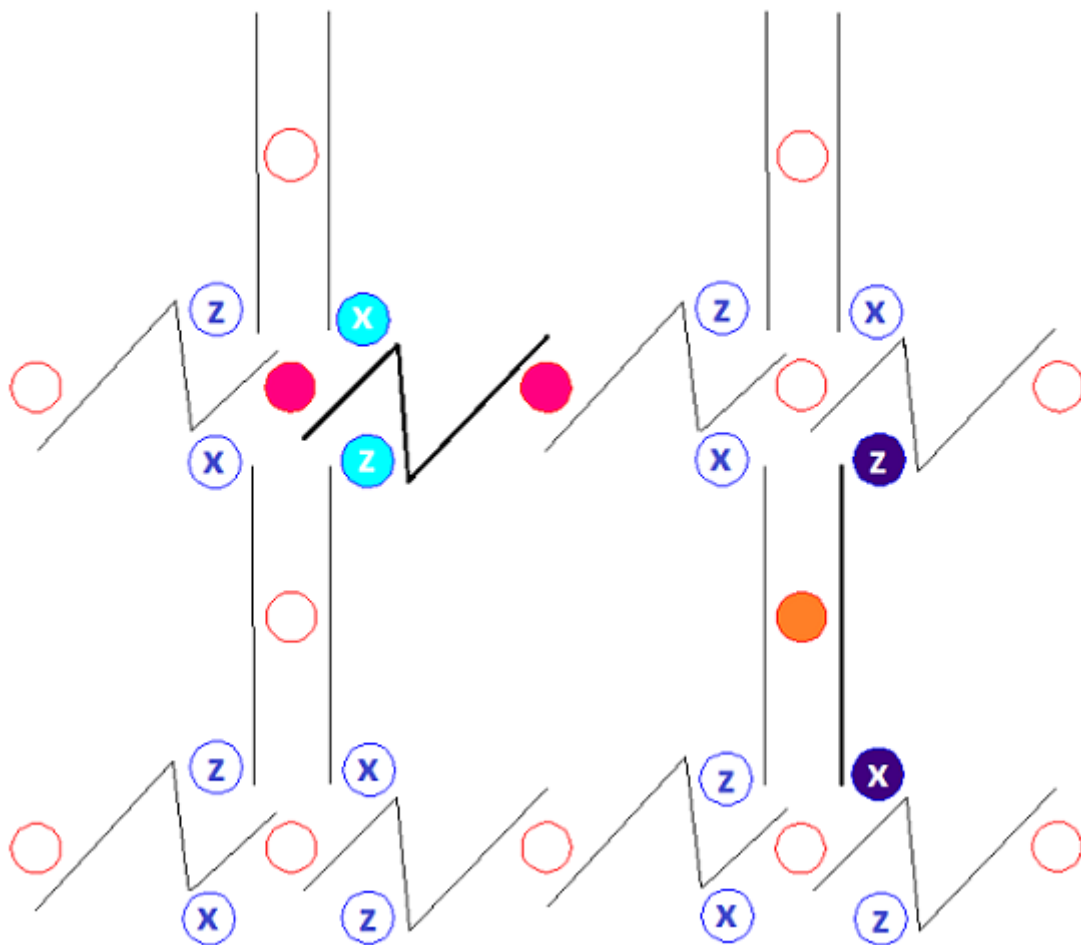


Figure 10: A way of representing the code in an abstract geometric layout. Ancillas are shades of blue, computational qubits are shades of red, transmission lines are black. To illustrate how the connections work, the bold transmission line on the left connects both magenta computational qubits and cyan ancillas. The bold transmission line on the right connects the orange computational qubit and violet ancillas.

To convert this abstract picture into an actual building plan, there are additional conditions. The length of the transmission lines has to be about 1 cm, so that the resonant

frequency is in the GHz range, while the qubits should be as close together as possible. The solution to this is to use winding lines instead of straight ones. There also has to be space for the flux bias lines next to each qubit, to allow them being tuned. Dimensions for the lines were taken from [4][5][8]. My solution is shown in Fig. 14. The length of each transmission line is between 1 and 2 cm, allowing for a resonant frequency in the required range. In addition, the length of two neighbouring lines is never the same, as to prevent unwanted coupling effects.

There are three different kinds of qubits regarding their positions on the transmission lines: One kind is at the end of both lines connecting to it, as shown in Fig. 11.

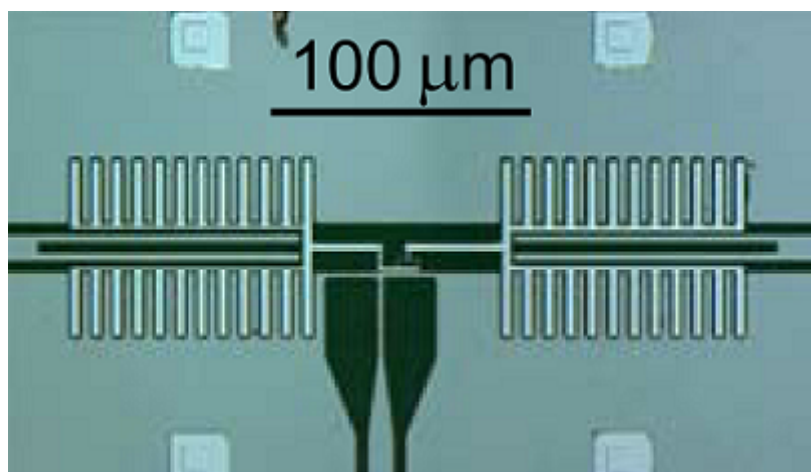


Figure 11: From [5]. A transmon connected to the end of two transmission lines. It is not entirely clear where the capacitance parallel to the Josephson junction lies (see Fig. 5).

Its design has been taken from [5]. In Fig. 10 the magenta qubits are examples of this type.

The second kind sits in the middle of both lines. The design is shown in Fig. 12 and takes care that the different transmission lines should not get closer to each other than about $100 \mu m$. Because of this restriction and the geometry of the layout an L-shape for the qubit has been used. In Fig. 10 the orange qubit is an example of this.

The third kind is exclusive to ancillas and has one transmission line ending at the qubit and the other one passing along. It is shown in Fig. 13. All ancillas are of this type.

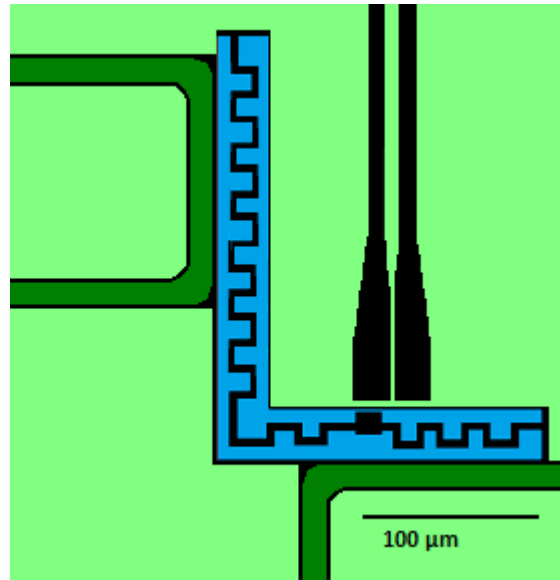


Figure 12: L-shaped transmon. Two different transmission lines (dark green) pass it.

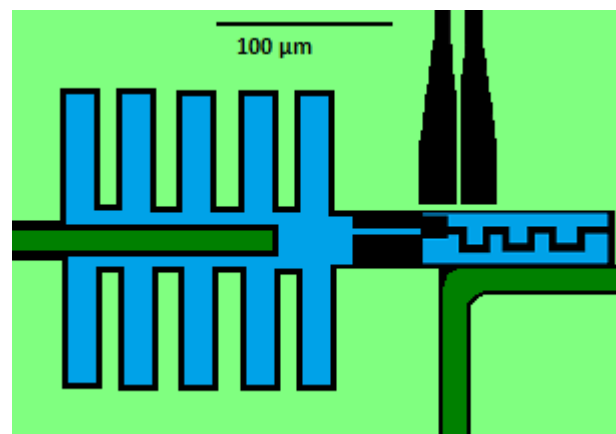


Figure 13: Third type of transmon. It is a hybrid of the first two types. One transmission line coming from the left ends here, while another transmission line passes at the bottom. All ancillas look like this.

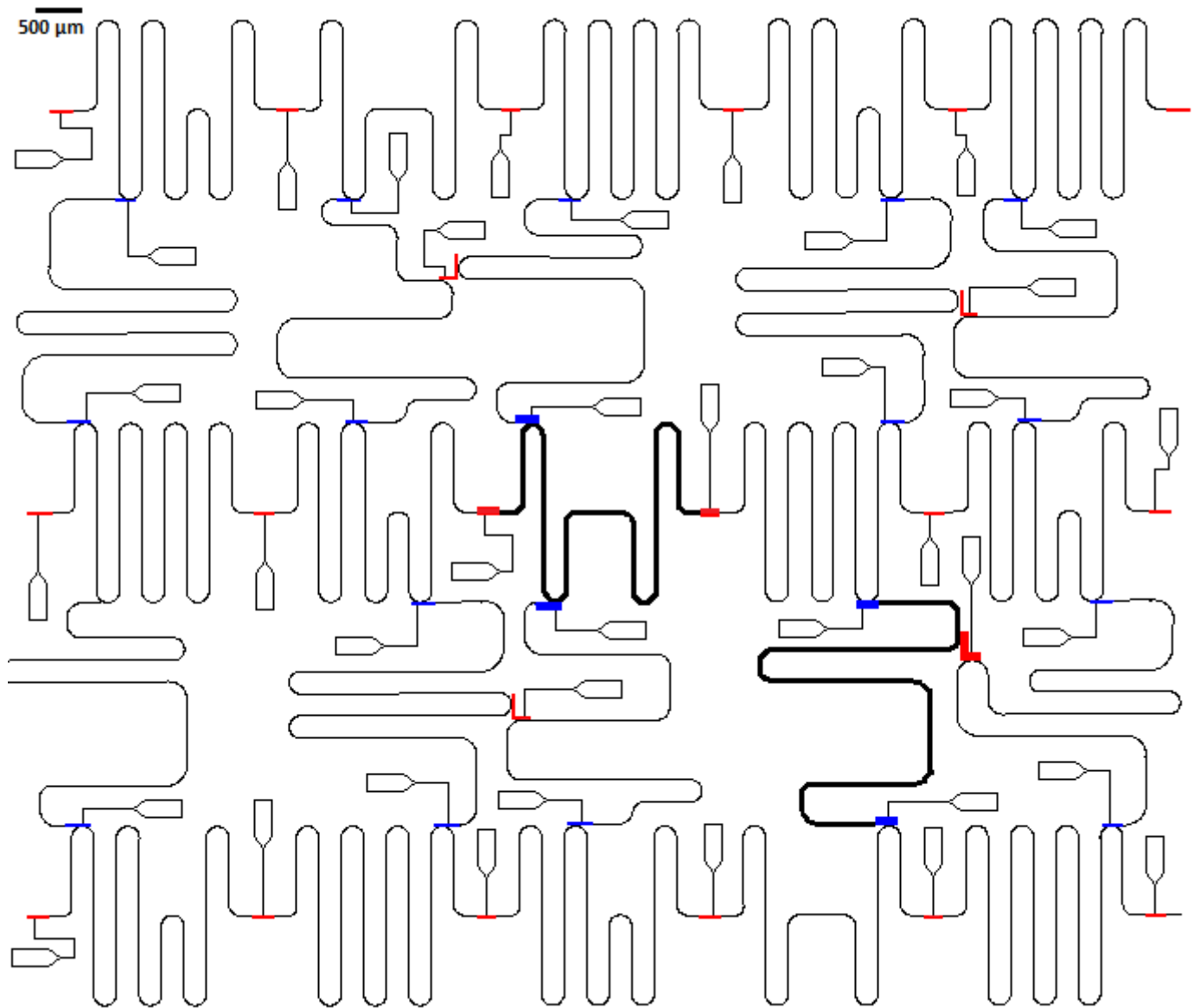


Figure 14: Circuit based on the triangular code. Ancilla qubits are coloured blue; computational qubits are coloured red. There are flux bias lines leading to every qubit. In the center, marked in bold, there is one transmission line together with its associated qubits. These qubits are equivalent to the magenta and cyan qubits in Fig. 10. On the bottom right, marked in bold, there is one transmission line together with qubits equivalent to the orange and violet qubits in Fig. 10. The flux bias lines actually have rounded corners to minimize reflection, as opposed to the right-angled corners shown here due to resolution.

5 Example of a Measurement Round in the Triangular Code

To perform any actions on the qubits, flux pulses have to be applied to them. These pulses allow the execution of 1 and 2-qubit gates. For 1-qubit gates, the pulses apply rotations of the state in the Bloch sphere. The amplitude of the pulse is proportional to the angle of the rotation. It is possible to differentiate between the different rotational axes through the phase of the pulse applied. Typically Gaussian envelopes are used for the pulses, cut off after $\pm 2\sigma$, limiting the length of the pulse to a few ns. The actual measurement of the ancillas takes much longer, in the order of magnitude of 1 μs [4][8]. The only 2-qubit-gates that are used here are the controlled-Z gates. They are realised by the longer, rectangular shaped pulses. The length τ of those pulses is determined by the equation $\zeta \cdot \tau = \pi$, where ζ is defined as in chapter 3. τ is about 10-20 ns. The amplitude of the pulses depends on the qubits involved in the gate.

To measure an Hermitian and unitary operator U with two eigenvalues, like the X or Z operator, one needs to apply the following circuit:

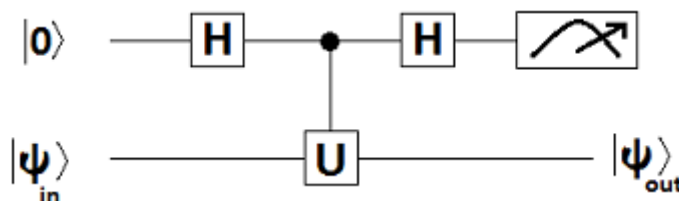


Figure 15: Adapted from [1]. The measurement yields one of the two states $|0\rangle$ or $|1\rangle$, indicating an eigenvalue of the operator U . $|\psi_{out}\rangle$ is the eigenvector corresponding to that eigenvalue.

If $|\psi_{in}\rangle$ is an eigenvector of U , the measurement result corresponds to the eigenvalue associated with that eigenvector. If $|\psi_{in}\rangle$ is not an eigenvector of U , it can still be projected onto the two eigenvectors of U . Measurement then yields a result which will suggest the first of those eigenvectors some of the time, and the second otherwise. In any case, $|\psi_{out}\rangle$ is the eigenvector which corresponds to the eigenvalue that was found in the measurement. For example, to measure the value of a Z-operator on a state, one can use the circuit shown in Fig. 16, which is equivalent to the one above for $U = Z$, using the equivalence from Fig. 2. Measurement of the ancilla will obtain a result of $|0\rangle$ if $|\psi_{in}\rangle = |0\rangle$ and $|1\rangle$ if $|\psi_{in}\rangle = |1\rangle$. If $|\psi_{in}\rangle$ is a different state, for example $|\psi_{in}\rangle = \frac{1}{\sqrt{2}}(|0\rangle + |1\rangle)$, the ancilla would be measured as being in the state $|0\rangle$ half the time and being in the state $|1\rangle$ the other half. In the first case, $|\psi_{out}\rangle$ would be $|0\rangle$ and in the second case it would be $|1\rangle$.

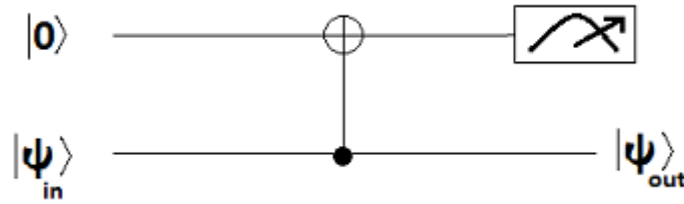


Figure 16: Measurement of the state of the Z-Operator using a CNOT

For transmon qubits realized in experiments, typically c-Phase gates are used [4][8]. They can be used to execute controlled-Z gates. A circuit measuring an X-operator using a controlled-Z looks like this:

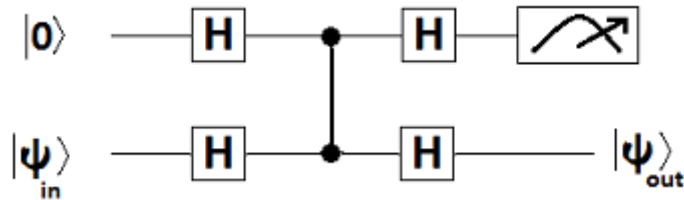


Figure 17: Measurement of an X operator using controlled-Z gates instead of CNOT.

The following contains an example of one measurement round used in detection errors in the triangular code. Used here are a total of 5 computational qubits and two ancillas, one each for the X and Z syndrome measurement, see Fig. 18. The order in which the actions are performed has been taken from the protocol outlined in [2]. The abstract sequence of gates can be found in Fig. 19. Note that some of them can be carried out simultaneously, as they involve qubits which will never couple together. In case where the state of a qubit is $|0\rangle$, one does only need to apply a $\frac{\pi}{2}$ rotation about the y-axis instead of a whole Hadamard-gate as those are equivalent in this situation. This is the case here for the ancillas at the start of the process, as they are prepared in the $|0\rangle$ state before the measurement begins.

Fig. 20 shows how an actual sequence of pulses could look like.

Depending on the result of the measurement, errors of the qubits can be detected. There are four possible measurement outcomes for the x and z ancilla combined, with each result indicating a different kind of error (or the absence of errors). Note that the result of this measurement is not absolute - even though there could be no errors detected by these two ancillas, there are still some combinations of errors possible. With additional ancillas the kind of error and the location of the erroneous qubits can be detected, and appropriate actions can be performed on those qubits to bring them back into the desired state.

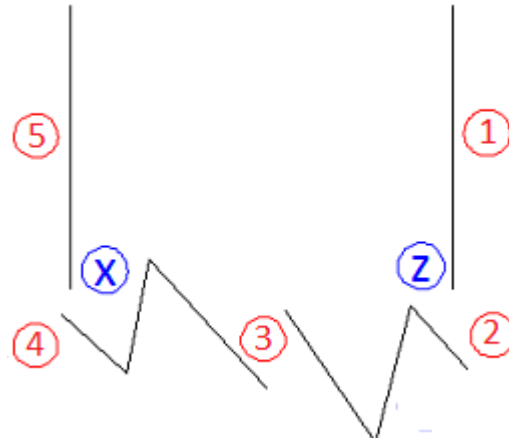


Figure 18: The qubits used in the following measurements, five computational qubits (red) and two ancillas (blue). Qubit 3 connects to both ancillas and takes part in both syndrome measurements.

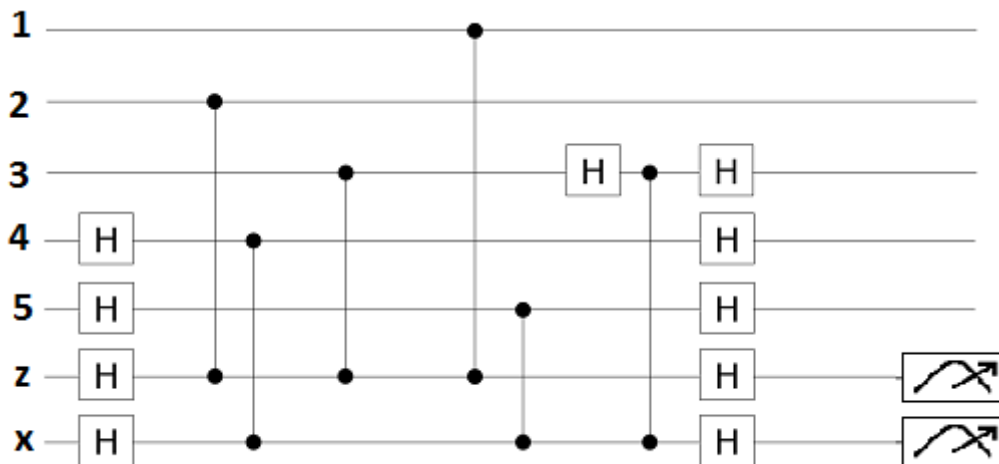


Figure 19: Abstract sequence of pulses.

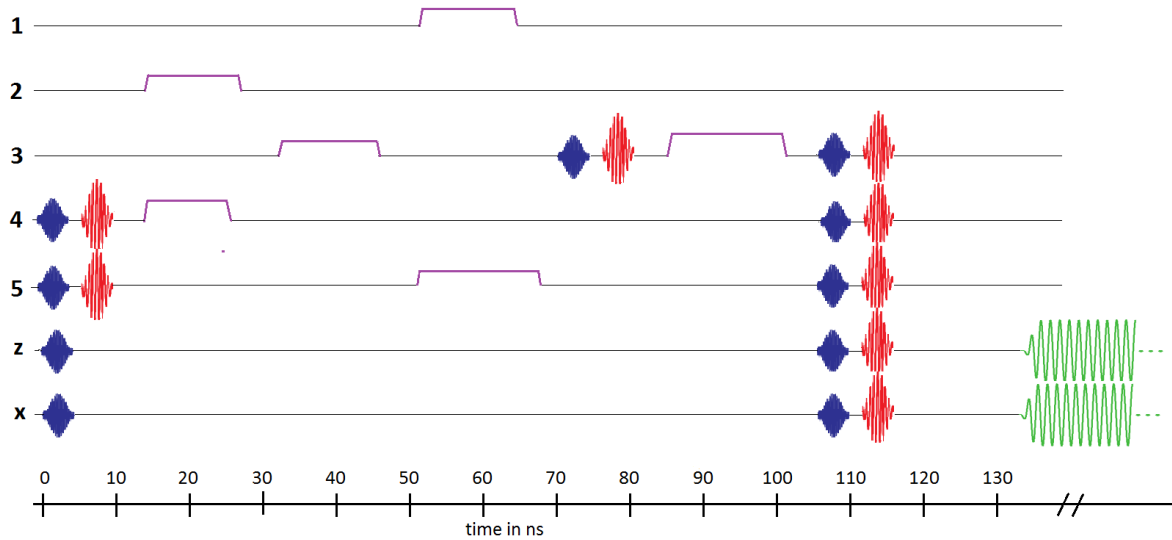


Figure 20: Pulse sequence for performing the syndrome measurement, adapted from [4]. Blue pulses mean $\frac{\pi}{2}$ rotations about the y-axis, red pulses mean π rotations about the x-axis. The amplitude of the red pulses is higher because of the larger rotation. Rectangular purple pulses are responsible for performing c-Phases. Their length is dependent on the energy gap due to the avoided crossing, their amplitude on the frequencies of the qubits which are supposed to be involved in the gate. At the end, the two ancillas are measured (green); the actual measurement takes much longer than the pulse sequences before.

References

- [1] Michael A. Nielsen and Isaac L. Chuang, Quantum Computation and Quantum Information, Cambridge University Press, 2000
- [2] S. Bravyi, Topological subsystem codes with 3-qubit checks, unpublished
- [3] http://en.wikipedia.org/wiki/Bloch_sphere
- [4] L. DiCarlo, J.M. Chow, et al., Demonstration of Two-Qubit Algorithms with a Superconducting Quantum Processor, arXiv:0903.2030v2
- [5] B.R. Johnson, M.D. Reed, et al., Quantum Non-demolition Detection of Single Microwave Photons in a Circuit, arXiv:1003.2734v1
- [6] N. David Mermin, Quantum Computer Science: An Introduction, Cambridge University Press, 2007
- [7] H. Paik, D.I. Schuster, et al, How coherent are Josephson junctions?, arXiv:1105.4652v2
- [8] L. DiCarlo, M.D. Reed, et al., Preparation and Measurement of Three-Qubit Entanglement in a Superconducting Circuit, arXiv:1004.4324v1

Acknowledgement

I would like to thank Prof. DiVincenzo for his guidance on this project and for being a patient teacher.

Hiermit versichere ich, dass ich diese Arbeit selbstständig verfasst und keine anderen als die angegebenen Quellen und Hilfsmittel benutzt habe, sowie Zitate kenntlich gemacht habe.

Aachen, den 11. Juni 2012

Dennis Huben